

ARTICLE



Immunophenotypic and molecular characterization of pancreatic neuroendocrine tumors producing serotonin

Thomas Depoilly^{1,2}, Raffaele Leroux³, Dafne Andrade⁴, Remy Nicolle⁵, Marco Dioguardi Burgio⁵, Ilaria Marinoni⁶, Safi Dokmak⁷, Philippe Ruzsniowski⁸, Olivia Hentic⁸, Valérie Paradis^{1,3}, Louis De Mestier^{3,8}, Aurel Perren⁶, Anne Couvelard^{1,3} and Jérôme Cros^{1,3}✉

© The Author(s), under exclusive licence to United States & Canadian Academy of Pathology 2022

Serotonin producing pancreatic neuroendocrine tumors (SP-PanNET) account for 0.58–1.4% of all pancreatic neuroendocrine tumors (PanNET). They may present with atypical symptoms, such as acute pancreatitis and are often radiologically characterized by main pancreatic duct dilatation. SP-PanNET are well differentiated neuroendocrine tumors (NET) distinct from classical PanNET by atypical serotonin secretion and abundant dense stroma deposition, like serotonin producing ileal NET leading in some cases to difficulties to reliably distinguish SP-PanNET from ileal NET metastases. The biology and molecular profile of SP-PanNET remain poorly characterized and the cell of origin within the pancreas is unclear. To address these questions, we analyzed a large cohort of SP-PanNET by immunohistochemistry ($n = 29$; ATRX, DAXX, MENIN, Islet1, PAX6, PDX1, ARX, CDX2), whole genome copy number array (Oncoscan™) and a large NGS panel (NovoPM™) ($n = 10$), FISH ($n = 13$) and RNA sequencing ($n = 24$) together with 21 ileal NET and 29 nonfunctioning PanNET (NF-PanNET). These analyses revealed a unique genomic profile with frequent isolated loss of chromosome 1 (14 cases-61%) and few pathogenic mutations (*KMT2C* in 2 cases, *ARID1A* in 1 case). Unsupervised RNAseq-based clustering showed that SP-PanNET were closer to NF-PanNET than ileal NET with an exclusive beta cell-like signature. SP-PanNET showed TGF- β pathway activation signatures associated with extracellular matrix remodeling and similar signature were reproduced in vitro when pancreatic stellate cells were exposed to serotonin. SP-PanNET immunohistochemical profile resemble that of ileal NET except for PDX1 and PAX6 expression to a lesser extent suggesting that these two markers may be useful to diagnose SP-PanNET. Taken together, this suggests that SP-PanNET are a very specific PanNET entity with a peculiar biology leading to the characteristic fibrotic aspect.

Modern Pathology (2022) 35:1713–1722; <https://doi.org/10.1038/s41379-022-01110-x>

INTRODUCTION

Serotonin-producing neuroendocrine tumors in the pancreas (SP-PanNET) were first described in 1963¹. These rare tumors account for 0.58–1.4% of all pancreatic neuroendocrine tumors (PanNET)², despite an underestimated prevalence and incidence because most cases are not associated with clinical carcinoid syndrome³. In addition, serotonin expression is not usually assessed in PanNET. Similar serotonin-producing NET were also reported in the lung⁴. Patients with localized SP-PanNET may be asymptomatic or display misleading symptoms and imaging, such as severe abdominal pain, acute pancreatitis and duct dilatation⁵. Carcinoid symptoms, including flush, diarrhea, asthma or heart valve lesions, have been observed essentially in tumors with liver or retroperitoneal metastases³. Abdominal computed tomography classically shows hyper enhanced well delineated lesions in arterial phase acquisitions with main pancreatic duct stenosis and upstream dilatation^{5,6}. This subtype of NET is distinct from the

remaining PanNETs by its serotonin expression, easily identified by immunohistochemistry and also by the presence of a very dense fibrotic pauci-cellular stromal reaction that often leads to main duct compression, a highly unusual feature in PanNET. Serotonin expression and the presence of a desmoplastic stroma are also key characteristics of ileal NET. The latter may metastasize to the pancreas and distinguishing them from SP-PanNET may be very challenging and carry important therapeutic consequences⁷.

Two aspects of SP-PanNET remain particularly unclear: (i) what is the cell of origin within the pancreas and what are the molecular alterations driving them and (ii) what is responsible for the massive desmoplastic stroma in these tumors. Molecular alterations described in non-functioning PanNET (NF-PanNET), implicate chromatin remodeling genes like *MEN1* or *ARID1A*, upregulation of *TERT* or dysregulation of *DAXX* and *ATRX* that are involved in telomere maintenance and inactivation of *PTEN* or *TSC2* leading to PI3K/mTOR pathway activation⁸. Chromosomal alterations of NF-

¹Université Paris Cité - APHP Hôpital Beaujon/Bichat, Department of Pathology, FHU MOSAIC, 100 Boulevard du Général Leclerc, 92110 Clichy, France. ²Faculté de Médecine, Sorbonne-Université, 15 rue de l'École de Médecine, 75006 Paris, France. ³INSERM U1149—Team 9, APHP-Hôpital Beaujon, 100 Boulevard du Général Leclerc, 92110 Clichy, France. ⁴Department of Pathology, Grupo Fleury, São Paulo, Brasil. ⁵Université Paris Cité - APHP Hôpital Beaujon, Department of Radiology, FHU MOSAIC, 100 Boulevard du Général Leclerc, 92110 Clichy, France. ⁶Institute of Pathology, University of Bern, Murtenstrasse 31, 3008 Bern, Switzerland. ⁷Université Paris Cité - APHP Hôpital Beaujon, Department of Hepatobiliary and Pancreatic Surgery, 100 Boulevard du Général Leclerc, 92110 Clichy, France. ⁸Université Paris Cité - APHP Hôpital Beaujon, Department of pancreatology, FHU MOSAIC, 100 Boulevard du Général Leclerc, 92110 Clichy, France. ✉email: jerome.cros@aphp.fr

Received: 16 February 2022 Revised: 12 May 2022 Accepted: 12 May 2022
Published online: 23 June 2022

PanNET are loss of chromosomes 1q, 3p, 11q and gain of 7p and 9q⁹. In contrast, molecular studies of ileal NET demonstrated isolated loss of chromosome 18 where tumor suppressor genes *SMAD2* and *SMAD4* are located and in some cases gain of chromosome 14 with a pejorative prognostic mutation in *CDKN1B*⁹. Nevertheless, the origin and molecular alterations driving SP-PanNET are largely unknown, especially how this massive desmoplastic stroma is produced. FISH studies showed monosomic chromosome 18 loss similar to ileal NET but different immunohistochemical pattern¹⁰.

Numerous studies showed a link between the secretion of serotonin, whether from tumor or during inflammation/tissue repair processes, and the development of fibrosis in various organs (mesenteric, pulmonary, cardiac or liver)^{11–16}. This secretion appears to be associated with the fibrotic stroma, although it is not found in all sclerosing PanNET¹⁷ nor in all pulmonary NETs with a fibrous appearance⁴. The role of TGF- β also appears central, as some studies highlighted an activation of its downstream signaling pathways in these fibrotic pathologies^{11,13,16,18,19}.

The aim of this study was to describe the molecular landscape of SP-PanNET and decipher their origin together with testing an immunohistochemical panel to distinguish them from ileal NET metastases.

MATERIALS AND METHODS

Patients and samples

This study was performed according to Helsinki declaration. The study was approved by local Institutional Review Board (CEERB Paris Nord, IRB 00006477-15-073). We reviewed the surgical pathology files of Beaujon Hospital Department of Pathology for patients with a diagnosis of SP-PanNET from 2004 to 2020, defined by high and diffuse serotonin immunohistochemical expression. A representative formalin-fixed, paraffin-embedded tissue block from each case was selected (26 resection specimen and 3 biopsies). As control groups for the RNA sequencing study, we selected 21 ileal NET (15 G1, 6 G2) and 29 NF-PanNET (16 G1, 13 G2). For the immunohistochemistry study we used a different set of tumors that were on already constructed TMA of ileal NET ($n = 42$) and NF-PanNET ($n = 35$).

To subclassify the histopathologic architecture of SP-PanNET, we used the criteria proposed by previous studies²⁰: solid sheets of cells with surrounding stromal fibrosis and/or trabecular-glandular architecture with interspersed stromal fibrosis. The first type is characterized by solid nests and sheets of neoplastic cells separated by fibrous tissue bands but without the peripheral palisading seen in ileal NETs. The thickness of the fibrous bands differed from area to area, and the total amount of fibrosis was generally less than 50% of the total tumor area. The second type is characterized by small trabecular-glandular or purely trabecular arrangements of neoplastic cells that are surrounded and spaced apart by diffusely developed fibrotic tissue. The total amount of fibrosis generally exceeded 50% of the total tumor area. The following pathological data were also collected: tumor grade (G1 to G3) and tumoral differentiation (well or poorly differentiated) according to the 2017 World Health Organization classification²¹, Ki-67 count (%), the presence of metastatic lymph nodes, and the presence of microvascular and perineural invasion. Patient survival data and clinical information were obtained from our surgical/clinical database.

Copy number alterations / Genomic profiling

Microdissection of the tumor area was performed to obtain DNA from SP-PanNET using the Qiagen QiaAMP FFPE according to the manufacturer instructions (Qiagen[™], Hilden, Germany). Sample concentration was assessed using a Quantifluor[®] dsDNA ONE fluorometer (Promega[™], Madison, WI, USA), according to the manufacturer's instructions. The genomic profile (copy number, gains, loss and loss of heterozygosity) was obtained with OncoScan[™] arrays according to the supplier recommendations (ThermoFisher ONCOSCAN CNV FFPE ASSAY, ref. 695,902), as described previously²². The OncoScan assay uses molecular inversion probe (MIP) technology, which interrogates 220,000 regions in the genome with a 50 to 100 kb copy number resolution in 900 oncogenes and a 300 kb genome-wide copy number resolution outside oncogenes. Data analysis was performed using Chromosome Analysis Suite Software from Affymetrix (CHAS), version 3.0.0.42 with annotations na33.2 (hg19). QC

metrics were generated and gave information about the data quality and the level of chromosomal aberrations.

FISH

Sections of 3 μ m were cut. To investigate chromosome 1 and 18 losses, we used a mixture of 2 probes, one specific for the *MALT1* gene on chromosome 18 and one specific for chromosome 1 centromere. FISH was performed as follow: after deparaffinization and dehydration the slides were left 25 min at 80 °C in the specific pre-treatment solution, then washed with 2x standard saline citrate (SSC). In total, 10 ml of the FISH probe were spotted on hydrophobic gel bond film and mounted on a glass slide. The samples were denatured at 74 °C for 10 minutes and incubated 72 h at 37 °C in a humid box. The slides were then washed progressively in 2x SSC at room temperature, 2x SSC / 0.3% NP-40 at 73 °C and again in 2x SSC at room temperature. Finally, counter stain with DAPI was performed. FISH results were evaluated using an Olympus VS 110 Fluorescent Scanner (Olympus, Volkstetwil, Switzerland), assessing at least 100 nuclei per case.

Mutational analysis

The same DNA was used to assess the mutational status of 484 genes using the NovoPM[™] 2.0 panel (Novogene in house sequencing (detail available upon request), Sacramento, CA, USA). This panel assessed single nucleotide variant (SNV), indel, copy number variation (CNV), tumor mutational burden (TMB), microsatellite instability (MSI) and a 43 genes panel to detect fusion genes. Variant were detected and filtered using the following parameters: exonic or splicing localization, frequency <0.1% in the 1000 Genomes and Exac databases, non-synonymous variants, depth of coverage >15 and allelic ratio >5%^{23,24}. Prediction of pathogenicity was based on CADD score >0.025, or if unavailable, on M-CAP score >15, SIFT score <0.05 and/or Polyphen-2 score >0.9, and visual^{25,26}.

Situ Hybridization analysis

RNA-sequencing. Total RNA was extracted using RNeasy FFPE kit (Qiagen[®], Hilden, Germany) for the tumors and the RNA storm kit (Cell data, CA USA) for the PS1 cell line. RNA library were prepared using the Lexogen QuantSeq 3' mRNA-Seq Library Prep Kit FWD and sequenced on a Illumina Novaseq to a minimum depth of 50 million reads generated for each sample. Raw fastq files were probed for sequencing quality control using FastQC. Sequencing reads were mapped to human transcripts corresponding to human hg38 genome (hg19 version) and transcript annotation (Ensembl 75) using RSEM with default parameters (or STAR) with the proposed ENCODE parameters. RSEM package was used to prepare the reference genome with given GTF and calculated expression from mapped BAM files. STAR aligner was used to map reads in RSEM algorithm. Transcripts mapped data were normalized to counts per million from RSEM and log2 transformed.

Principal Component analyses (PCA) and unsupervised hierarchical clustering were carried out using Clustvis²⁷. Unsupervised clustering was performed on log2-transformed data using Euclidean distance metric and Ward method. DeSeq2 on raw count was used to identify differentially expressed genes between groups²⁸. Gene Set Enrichment Analysis (GSEA) method was used to analyzed the pathways enriched in each group²⁹.

Cell line

The PS1 cell line (hTERT immortalized pancreatic stellate cells) were grown in DMEM F12 Advanced Ham's (Gibco, USA) with 10% fetal calf serum and 1% Penicillin/Streptomycin and 1% L-glutamine³⁰. For the RNA sequencing experiment, PS1 were treated for 24 h with serotonin (5-Hydroxytryptamine, 3-(2-Aminoethyl)-5-hydroxyindole, Selleckchem, UK) at 0.1 μ M or the vehicle. To assess the effect of serotonin on cell growth, PS1 were gradually serum-deprived (fetal calf serum 5% for 24 h and 0% for 24 h) before exposition with serotonin at 0.1 μ M or vehicle for 24 h. Cell viability was assessed by fluorescence using the Presto Blue reagent (Thermo Fisher Scientific, Waltham, MA, USA). Experiments were performed in sextuplicate.

Staining and Immunohistochemistry

Picrosirius stain was performed as previously described³¹. Fibrotic stained areas were assessed using a computer-assisted quantification and reported as the percentage of positive pixels in the tumor area (Aperio Pixel+ algorithm). Immunohistochemistry were performed on 3 μ m thick sections using routine automats (Nexus GX, Ventana) with the following antibodies (serotonin, DAXX, ATRX, PAX6, PDX1, ISLET1, CDX2, ARX, and MEN1) (See

Table 1. Patients characteristics.

Patient No	Sex	Years	Symptoms	Somatostatin analog scintigraphy Pos/Neg	Tumor size (cm)	Ki67	Grade	Metastases	Follow-up (mo)
1	F	71	AD	NA	1,2	4	G2	N	138
2	M	81	A	P	2,7	4	G2	N	126
3	F	56	AP	N	1,8	1	G1	N	11
4	M	48	AP	NA	0,9	1	G1	N	26
5	M	56	AP	NA	1,2	1	G1	N	26
6	M	50	AP	P	1,5	3	G2	N	61
7	M	65	A	N (gallium)	2	1	G1	N	60
8	M	41	AD	N	0,8	1	G1	N	14
9	F	40	A	N (gallium)	0,7	1	G1	N	57
10	M	75	A	N	0,8	1	G1	N	22
11	F	60	AD/WL	N	0,8	1	G1	N	2
12	F	62	A	P (gallium)	1,5	1	G1	N	23
13	F	88	NA	NA	1	2	G1	NA	NA
14	M	62	DD	N (gallium)	0,6	1	G1	N	15
15	M	77	NA	NA	1,3	1	G1	NA	NA
16	M	54	A	P (gallium)	1,5	1	G1	N	3
17	F	61	A	NA	1	1	G1	N	8
18	M	45	ND	P (gallium)	3	1	G1	Y (synchronous)	46
19	F	63	A	P (gallium)	2,3	1	G1	N	14
20	F	64	NA	NA	1,6	2	G1	NA	NA
21	F	64	A	NA	1,5	1	G1	N	115
22	F	51	AP	N	0,7	2	G1	N	13
23	F	61	NA	NA	1,1	1	G1	NA	NA
24	F	62	NA	NA	1	1	G1	NA	NA
25	F	52	NA	NA	1,5	1	G1	N	119
26	M	70	NA	NA	3	2	G1	N	NA
27	M	59	A	NA	2,2	1	G1	N	93
28	F	58	AD	NA	2,5	1	G1	N	105
29	F	78	J	NA	0,8	1	G1	N	8

AD abdominal discomfort, A asymptomatic, AP acute pancreatitis, WL weight loss, DD decompensated diabetes, J jaundice

Supplementary Table 1 for clones and dilution details). To analyze serotonin, PAX6, PDX1, ISLET1, ARX and CDX2 expression, we assessed the percentage of stained cells. Cases were scored as negative (0: no positive cells), weakly positive (1: less than 10% of stained cell), heterogeneous positivity (2: 10 to 50% of stained cells) and diffuse homogeneous positivity (3: 50–100% of stained cells). For DAXX/ATRX/MENIN, the presence of the absence of the nuclear staining were recorded. To compare tumors from different localizations, we dichotomized the tumors as positive (score 1-2-3) or negative (score 0).

Statistical analyses

Categorical variables were expressed as frequencies (percentages) and compared using Chi-2 or Fisher's exact test. Continuous variables were expressed as median (interquartile range 25–75 [IQR]) and compared using Mann–Whitney U test. Overall survival (OS) was measured from the date of diagnosis and that of death, or the patient was censored at the date of last news. Median OS (and its 95% confidence interval [CI]) was estimated by the Kaplan–Meier method. Statistical analyses were performed using Prism® (v6, Graphpad™) software. A *p* value < 0.05 was considered as statistically significant.

RESULTS

Patients

Our cohort of SP-PanNET was composed of 29 patients (16 females) with a mean age of 61.2 years ± 11.6 (Table 1). Patients

did not show any symptoms of carcinoid syndrome. Seven patients showed unusual symptoms for NF-PanNET at diagnosis such as acute pancreatitis (*n* = 5/29), jaundice (*n* = 1/29) and uncontrolled diabetes. SP-PanNET were small (mean diameter = 1.46 cm ± 0.7), mostly grade 1 (mean Ki-67 = 1.41 ± 0.9%; three tumors were grade 2) and located throughout the pancreas. Follow up data were available for 23 patients. Median follow up was 26 months (IQR 13–77). No tumor-related death was recorded. One patient had a synchronous liver metastasis at diagnosis. Histologically, all SP-PanNET were well differentiated (Fig. 1). Most tumors showed a trabecular pattern (pattern B, *n* = 16) according to according to Soga and Tazawa^{10,32}. The remaining tumors had a nested pattern without the peripheral palisading as observed in ileal NET (pattern A, *n* = 8), or an equal mix of the two. The pattern was not assessed in the two biopsies. All except one lesion had extensive fibrotic stroma.

Genomic landscape

To assess whether SP-PanNET resemble ileal or NF-PanNET, ten SP-PanNET were analyzed with a whole-genome copy number microarray-based assay (Oncoscan™) and a large NGS panel. Summed chromosomal changes are summarized in Fig. 2 and individual profiles are shown in Supplementary Fig. 1. All tumor except one showed a rather stable genome. The most frequent

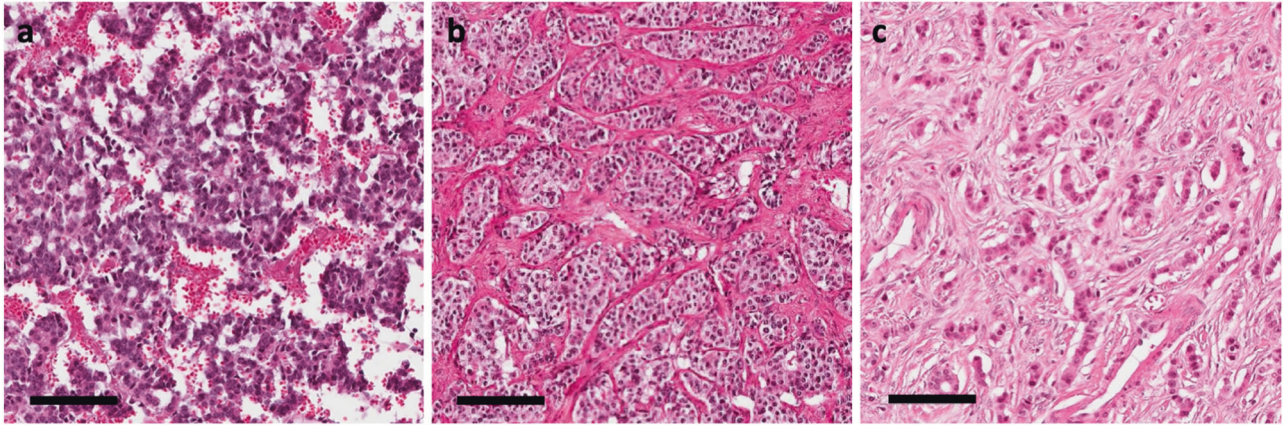


Fig. 1 Microscopic aspects of SP-PanNET compared to NF-PanNET. **a** Columnar pattern with no fibrotic stroma and abundant vascularization of a NF-PanNET (HES). **b** Nested pattern of a SP-PanNET (HES). **c** Trabecular pattern of a SP-PanNET (HES). Scale bar = 100 μ m.

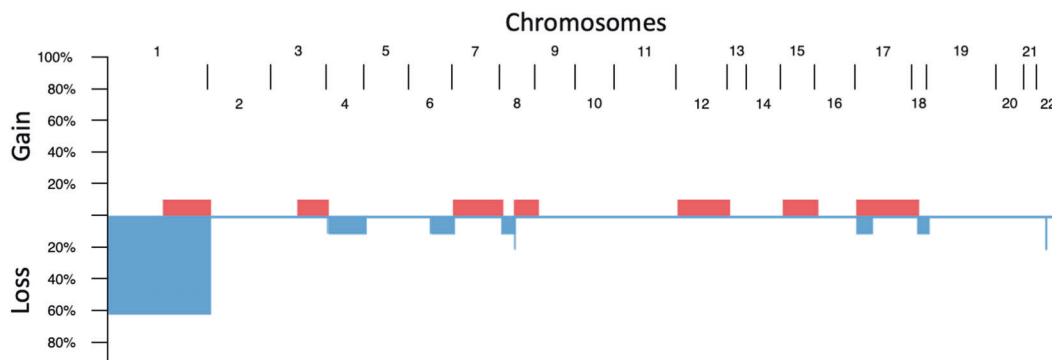


Fig. 2 Aggregated whole genome copy number of 10 SP-PanNET tumors. Chromosomal gains are represent in red and loss in blue together with the percentage of affected cases. The most frequent event is entire loss of chromosome 1 follow by partial or entire chromosomal gain or loss in few tumors.

chromosomal abnormalities were the loss of heterozygosity of the whole chromosome 1 ($n = 6/10$). This was an isolated finding in four cases, and in two cases it was associated with the loss of the whole chromosome 4 (subclonal loss in one of the 2 cases, not show in the summed figure). Other chromosomal changes were infrequent: partial loss of 6q ($n = 2$), 8p ($n = 2$), 8q ($n = 1$), 17p ($n = 1$), 18q ($n = 1$), 22q ($n = 1$), entire gain on chromosome 7 ($n = 1$), 12 ($n = 1$) or 15 ($n = 1$), partial gain on 1q ($n = 1$), 3p ($n = 1$), 8q ($n = 1$), 8p ($n = 1$) or 18p ($n = 1$). Two cases had no detectable chromosomal alteration. FISH analysis was performed on 13 additional cases with a chromosome 1 centromeric probe (*CEP1*) and a *MALT1* probe targeting chromosome 18. We found 8 additional cases (14/23 total; 61%) with a suspected loss of heterozygosity of chromosome 1 and one sample with a suspected loss in the chromosome 18 (with a normal chromosome 1 status). DNA sequencing revealed very few alterations. *KMT2C* was the most frequently mutated gene (2 cases: Stop gain c.906 T > A p.C302* and c.2722 G > T. p.G908C) although only in minor subclones (allelic frequency between 5 and 10%). One *ARID1A* indel was also present (c.3999_4001delGCA; p. Q1334del) and not associated with a loss of the other allele. No alteration was found on *ATRX*, *DAXX*, *MENIN*, *VHL*, *TSC1* and *TSC2* or *CDKN1C*. No MSI-high and no gene fusion were identified. Immunohistochemistry was performed in all 29 tumors and showed no abnormal staining for *DAXX* and *MENIN*. One tumor (2,5 cm) had an abnormal *ATRX* staining (case not sequenced). Taken together, these results suggest a clear difference between the genomic landscape of SP-PanNET and ileal NET. In addition,

SP-PanNET did not harbor the classical genomic abnormalities of NF-PanNET.

Origin and transcriptomic landscape

To gain further insights on SP-PanNET cell of origin and biology, we assessed the transcriptome of 24 SP-PanNET, 29 NF-PanNET and 21 ileal NET by RNA sequencing. Principal component analysis (PCA) clearly separated pancreatic NET (SP and NF) from ileal NET and showed a partial overlap between SP-PanNET and NF-PanNET (Fig. 3a). The first principal component separated the tumors according to their origin and the second principal component was less clear, separating ileal NET, SP-PanNET and a few PanNET from the rest of the PanNET. Proliferation index was not different between the two groups of PanNET suggesting that this second component is related to other biological functions. Further PCA analysis restricted to the pancreatic NET showed that NF-PanNET seemed more homogeneous than SP-PanNET and that these two entities still partially overlap (Supplementary Fig. 2a). Similar results were obtained with unsupervised hierarchical clustering based on the 1200 most variable transcripts. Ileal NET were grouped in a separate cluster from pancreatic NET. NF-PanNET were mostly grouped together in one cluster while SP-PanNET formed on large cluster subdivided in three sub group (Fig. 3b and Supplementary Fig. 2b). To further explore gene expression signatures of SP-PanNET and differences with NF-PanNETs, we performed a Gene Set Enrichment Analysis (Fig. 3c). SP-PanNET clearly showed a beta cell phenotype in contrast to NF-PanNET that expressed

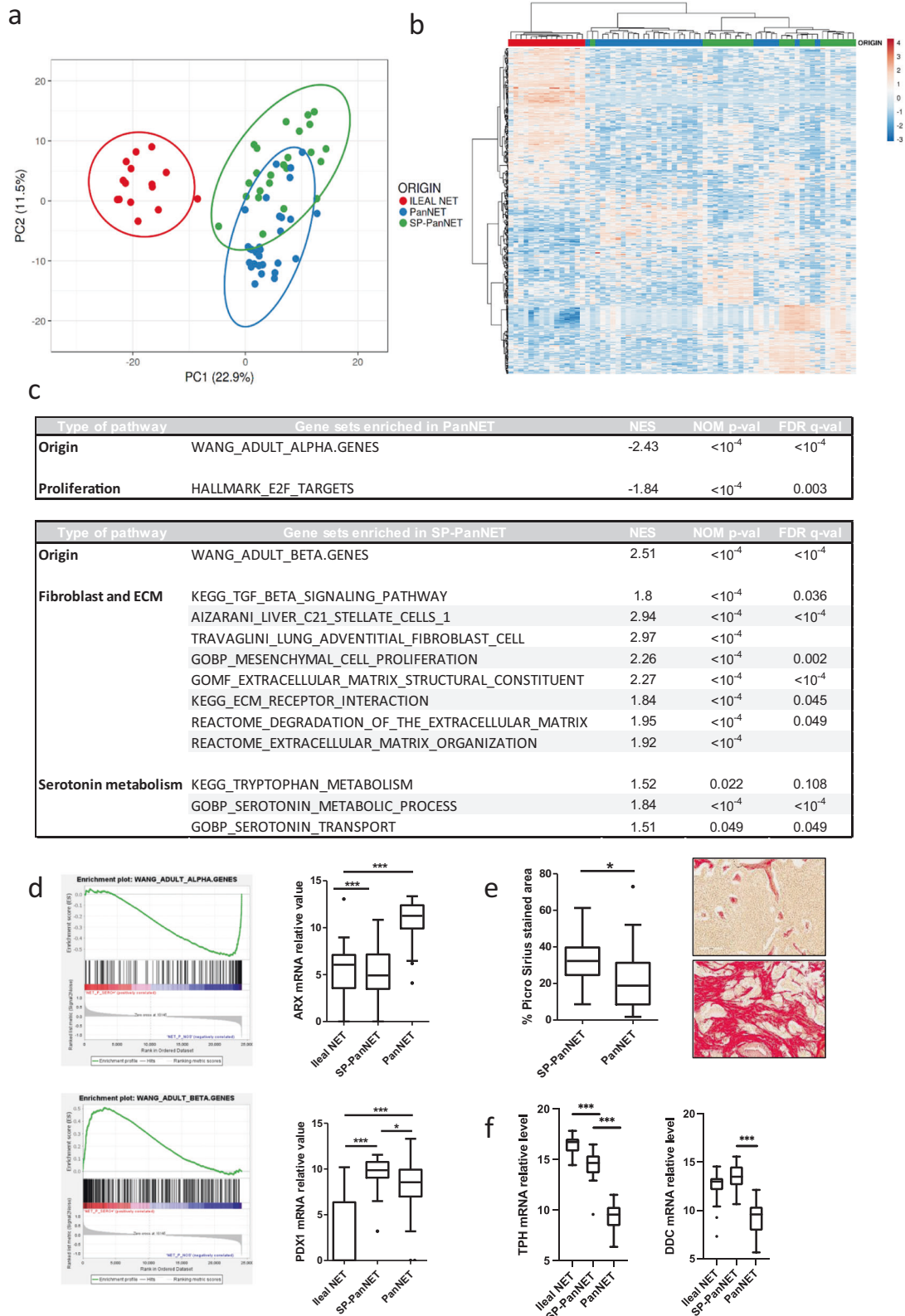


Fig. 3 Transcriptomic analysis of NET of SP-PanNET, PanNET and ileal NET. Principal component analysis (PCA) (a) and unsupervised hierarchical clustering (b) of 21 ileal NET (red), 24 SP-PanNET (green) and 29 Pan-NET (blue). c Gene Set Enrichment Analysis (GSEA) comparing PanNET and SP-PanNET. Pathways enriched in PanNET are in the top panel while pathways enriched in SP-PanNET are in the bottom panel (d) Enrichment of alpha and beta cell signatures in PanNET and SP-PanNET respectively together with ARX and PDX1 transcription factors mRNA relative values in SP-PanNET, Pan-NET and ileal NET. e Percentage of SP-PanNET and PanNET stained with picrosirius (automated computer-assisted quantification) and representative images (PanNET top panel and SP-PanNET bottom panel). f mRNA relative value of tryptophan hydroxylase (TPH) and the aromatic L-amino acid decarboxylase (DDC) in ileal NET, SP-PanNET and PanNET.

Table 2. Results of the immunohistochemical analysis of SP-PanNET, PanNET and ileal NET.

	SP-PanNET (n = 29)	PanNET (n = 35)	Ileal NET (n = 42)
ATRX			
Preserved expression	(27/28) 96,4% ^a	(27/30) 90%	(42/42) 100%
Loss of expression	(1/28) 3,6%	(3/30) 10% ^c	
DAXX			
Preserved expression	(29/29) 100%	(17/29) 58,6%	(42/42) 100%
Loss of expression		(12/29) 41,4% ^d	
MENIN			
Preserved expression	(26/26) 100% ^b	(20/34) 58,8%	(42/42) 100%
Loss of expression		(14/34) 41,2% ^e	
Islet1			
Negative	(24/29) 82,8%	(5/34) 14,7%	(42/42) 100%
Weak positivity	(5/29) 17,2%	(7/34) 20,6%	
Diffuse heterogeneous positivity		(8/34) 23,5%	
Diffuse homogeneous positivity		(14/34) 41,2% ^e	
PAX6			
Negative	(14/28) 50%	(15/34) 44,1%	(42/42) 100%
Weak positivity	(8/28) 28,6%	(6/34) 17,6%	
Diffuse heterogeneous positivity	(5/28) 17,9%	(5/34) 14,7%	
Diffuse homogeneous positivity	(1/28) 3,6% ^a	(8/34) 23,5% ^e	
PDX1			
Negative	(0/29) 0%	(11/34) 32,4%	(33/42) 78,6%
Weak positivity	(0/29) 0%	(7/34) 20,6%	(8/42) 19%
Diffuse heterogeneous positivity	(8/29) 27,6%	(5/34) 14,7%	(1/42) 2,4%
Diffuse homogeneous positivity	(21/29) 72,4%	(11/34) 32,4% ^e	
ARX			
Negative	(25/29) 86,2%	(6/34) 17,6%	
Weak positivity	(4/29) 13,8%	(5/34) 14,7%	
Diffuse heterogeneous positivity	(0/29) 0%	(9/34) 26,5%	
Diffuse homogeneous positivity	(0/29) 0%	(14/34) 41,2% ^e	
Serotonin			
Negative		(34/34) 100% ^e	
Diffuse homogeneous positivity	(29/29) 100%		(41/41) 100% ^f
CDX2			
Negative	(7/29) 24,1%	(3/34) 8,8%	(1/41) 2,4%
Weak positivity	(6/29) 20,6%	(3/34) 8,8%	
Diffuse heterogeneous positivity	(8/29) 27,6%		(40/41) 97,6%
Diffuse homogeneous positivity			

^an = 28.^bn = 26.^cn = 30.^dn = 29.^en = 34.^fn = 41.

higher level of alpha cell-related genes. In accordance, mRNA level of ARX, a key transcription factor for the maintenance of the alpha-like phenotype was low in SP-PanNET, at a level comparable to ileal NET (Fig. 3d). Immunohistochemistry gave similar results with only 4/29 SP-PanNET cases that displayed a weak positivity (Table 2). On the other hand, high level of PDX1 mRNA was specific to pancreatic-derived NET, consistently elevated in SP-PanNET while displaying various levels in NF-PanNET. Immunohistochemistry gave similar results with all 29 SP-PanNET displaying diffuse PDX1 positivity (Table 2). This

suggests that all SP-PanNET are of beta-like phenotype while NF-PanNET were of either alpha or beta-like phenotype. Other key pathways enriched in SP-PanNET were related to the desmoplastic stroma with TGF- β activation, fibroblast proliferation and remodeling of the extracellular matrix (Fig. 3c). Picrosirius staining showed significantly larger collagen deposits in SP-PanNET compared to NF-PanNET ($p = 0.02$) (Fig. 3e). Lastly, as expected, genes involved in tryptophan/serotonin metabolism and transport were upregulated in SP-PanNET. Particularly, the transcript level of the two key enzymes transforming tryptophan

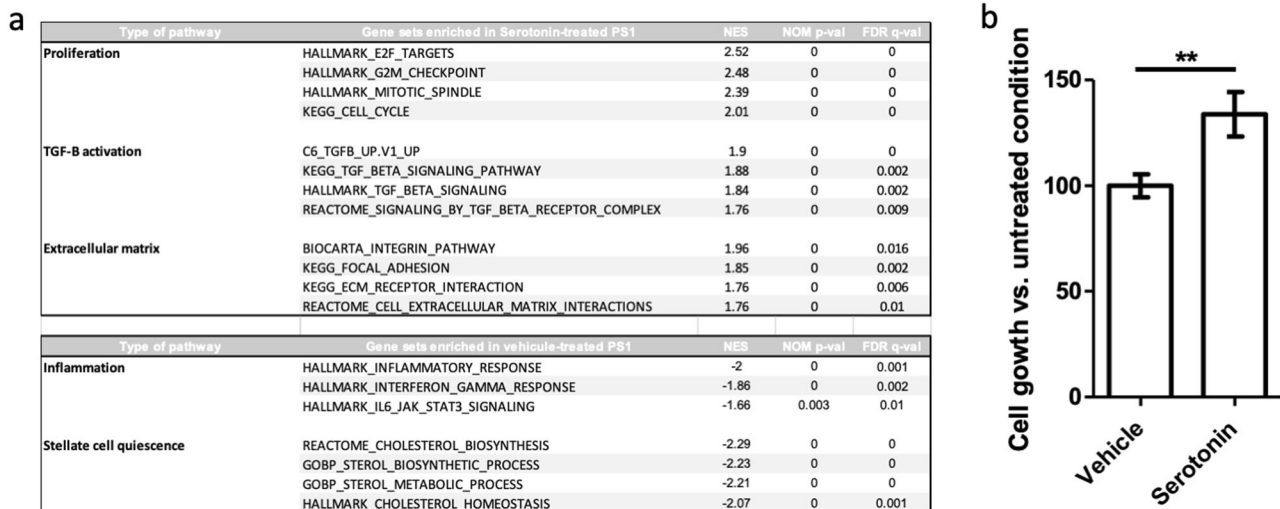


Fig. 4 Transcriptomic analysis of pancreatic PS1 stellate cells after serotonin stimulation. **a** Gene Set Enrichment Analysis (GSEA) comparing serotonin or vehicle treated PS1 cell line. Pathways enriched in serotonin treated PS1 are in the top panel while pathways enriched in the vehicle treated PS1 are in the bottom panel (**b**) Proliferation of PS1 in vitro when exposed 24 h to serotonin or vehicle.

into serotonin, namely the tryptophan hydroxylase (*TPH*) and the aromatic L-amino acid decarboxylase (*DDC*) were fairly similar in ileal NET and SP-PanNET and significantly higher than in NF-PanNET (Fig. 3f).

Role of serotonin in the desmoplastic stroma

To try to better understand the relationship between the tumor cell secretion of serotonin and the desmoplastic stroma in the pancreatic setting, we cultured hTERT-immortalized pancreatic stellate cells (PS1 cell line) with/without serotonin and assessed how it impacted their transcriptome (Fig. 4a). Gene Set Enrichment Analysis showed that serotonin exposition activated stellate cells, inducing their proliferation, TGF- β signaling and extracellular matrix production. In addition, serotonin decreased cholesterol metabolism and storage, a key feature of quiescent stellate cells. PS1 growth rate in vitro was significantly increased when serotonin was added to the culture media ($p = 0.022$) (Fig. 4b).

Distinguishing SP-PanNET from ileal NET in routine practice

Distinguishing SP-PanNET from ileal NET metastases located in the pancreas can be challenging, the latter not always being multiple or associated with liver simultaneous involvement. We performed an immunohistochemistry-based analysis on 29 SP-PanNET, 35 NF-PanNET and 42 ileal NET (Tables 2 and 3 and Fig. 5). When compared to NF-PanNET, SP-PanNET harbored a peculiar phenotype that may be confusing (Table 2). As described above, they show exceptionally abnormal staining for DAXX, ATRX or MENIN, markers that may be used to assign a pancreatic origin to a NET metastasis. In addition, SP-PanNET, rarely expressed ISLET-1 and always with a low intensity, a pattern different from NF-PanNET ($p < 0.001$). In contrast they often diffusely expressed CDX2, a rare occurrence in NF-PanNET ($p < 0.001$). PAX6 and PDX1 were more expressed in SP-PanNET compared to ileal NET ($p < 0.001$). PAX6 was a very specific marker (100%) but with a very low sensitivity (50%) while PDX1 was highly sensitive (100%) but with a lesser specificity (78%). Even if CDX2 was more frequently expressed in ileal NET, its high expression in SP-PanNET precluded its use to distinguish SP-PanNET from pancreatic ileal NET metastases.

DISCUSSION

We present here an integrated morphologic, genomic/transcriptomic and functional/immunohistochemical analysis of a very large cohort of rare pancreatic neuroendocrine tumors expressing

Table 3. Comparison of immunohistochemical markers between SP-PanNET, PanNET and ileal NET.

	SP-PanNET ($n = 29$)	PanNET ($n = 35$)	<i>P</i>
ATRX	1 (3,6%) ^a	3 (10%) ^c	0.612
DAXX	0 (0%)	12 (41.4%) ^d	<0.001
MENIN	0 (0%) ^b	14 (41.2%) ^e	<0.001
Islet1	5 (17,2%)	29 (85.3%) ^e	<0.001
PAX6	14 (50%) ^a	19 (55.9%) ^e	0.798
PDX1	29 (100%)	23 (67,6%) ^e	<0,001
ARX	4 (13,8%)	28 (82,4%) ^e	<0,001
Serotonin	29 (100%)	0 (0%) ^e	<0,001
CDX2	21 (72,4%)	6 (17,6%) ^e	<0,001
	SP-PanNET ($n = 29$)	Ileal NET ($n = 42$)	<i>P</i>
ATRX	1 (3,4%) ^a	0 (0%)	0,408
DAXX	0 (0%)	0 (0%)	1.0
MENIN	0 (0%) ^b	0 (0%) ^c	1.0
Islet1	5 (17,2%)	0 (0%)	0.009
PAX6	14 (50%) ^a	0 (0%)	<0.001
PDX1	29 (100%)	9 (21,4%)	<0.001
ARX	4 (13,8%)	0 (0%)	0,024
Serotonin	29 (100%)	41 (100%) ^d	1.0
CDX2	21 (72,4%)	42 (100%)	<0.001

^a $n = 28$; ^b $n = 26$; ^c $n = 30$; ^d $n = 29$; ^e $n = 34$.

^a $n = 28$; ^b $n = 26$; ^c $n = 14$; ^d $n = 41$.

serotonin. We demonstrated that they do not harbor the classical genomic abnormalities of NF-PanNET or ileal NET but instead often display an isolated loss of chromosome 1. Transcriptomic analysis revealed that they are closer to PanNET than ileal NET with an exclusive beta-like phenotype. The abundant stroma is probably linked to the activation of pancreatic stellate cells by serotonin leading to a TGF- β mediated deposition of extracellular matrix.

Genomic analysis revealed a chromosome 1 monosomy in 61% of cases, which has never been described before in SP-PanNET. La Rosa et al. described a monosomy of chromosome 18 like in ileal NET in all of the five cases that were studied using FISH. We could not confirm this finding using either FISH or whole genome array.

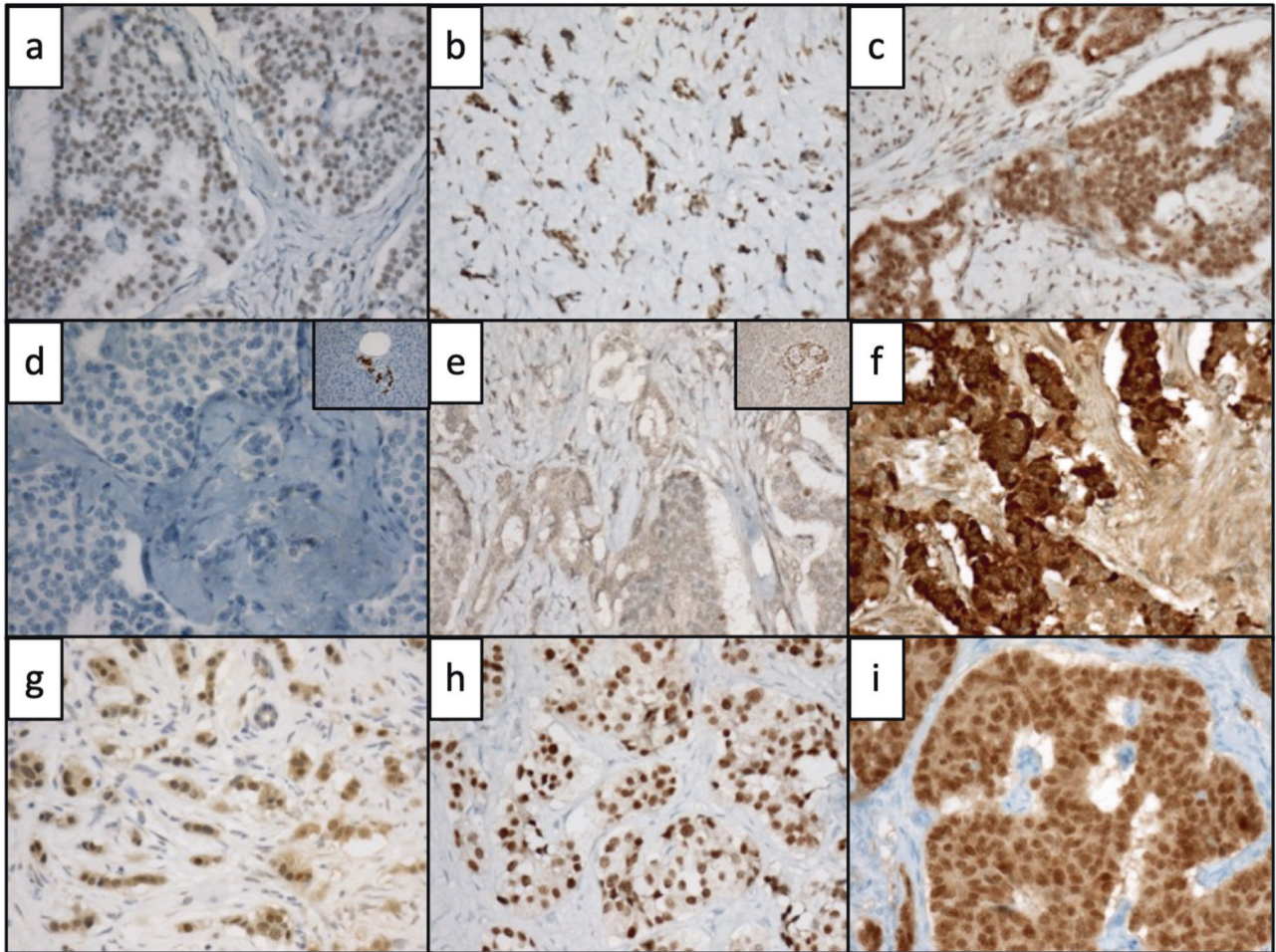


Fig. 5 Immunohistochemistry staining of SP-PanNET. a ATRX, (b) DAXX, (c) MENIN, (d) ARX Insert: normal endocrine islet, (e) Islet-1 Insert: normal endocrine islet, (f) Serotonin, (g) PAX6, (h) CDX2, (i) PDX1 ($\times 200$ magnification).

We did not find any mutation in *CDKN1B*, like in ileal NET⁹. This isolated chromosome 1 loss appears specific as it was not described in PanNET, even in small sized non-metastatic PanNET³³ and in insulinomas³⁴. Also, the absence of mutations in *MEN1*, *ATRX*, or *DAXX* cannot be related to the small size of SP-PanNET, as they may be found in <3 cm PanNET³³. Chromosome 1 contains numerous tumor suppressor genes. In NET, key genes involved in the tumorigenesis, like *MEN1* are often altered by mutation and/or copy number alteration. Here, except for *ARID1A*, we did not found recurrent pathogenic mutation in a gene located on chromosome 1. In contrast, we did find, albeit at low frequency, mutation in the lysine (K)-specific methyltransferase 2C (*KMT2C*) also known as mixed lineage leukemia 3 (*MLL3*). *KMT2C* is located on chromosome 7 and encodes a nuclear protein with DNA-binding domains and zinc finger type structures^{35,36}. This gene is often deleted in myeloid leukemias³⁵. *KMT2C* mutations are found in breast or gastric adenocarcinoma and neuroendocrine component of gastric MiNEN³⁵⁻³⁷. This suggests that like in other NET, the epigenetic (dis)regulation of genes have an important impact on carcinogenesis, an aspect that we did not tackle. Taken together these genomic results suggest that SP-PanNET are not superposable to ileal NET and have a specific carcinogenesis, without the key hallmark of NF-PanNET.

The transcriptomic profile of SP-PanNET was also closer to NF-PanNET than ileal NET, harboring an exclusive endocrine beta-like signature supporting the pancreatic origin. Indeed, the presence and role of normal serotonin secreting beta cells were recently

highlighted, including paracrine dialogue with (i) alpha cells to control glucagon production in low glucose conditions and (ii) vagal sensory axons^{38,39}. While these SP-PanNET may or may not originate from these particular cells, they recapitulate some of their features. In addition, serotonin was reported to favor normal endocrine beta cell proliferation in an autocrine manner during and after lactation suggesting that abnormal serotonin secretion by the tumor cells may sustain their growth⁴⁰. Of note, in our RNAseq data the 5-Hydroxytryptamine Receptor 2A (*SSTR2A*) mRNA level was similar in SP-PanNET and ileal NET and significantly much higher than in NF-PanNET (data not shown).

Another peculiar feature of SP-PanNET is their abundant desmoplastic stroma that may even outrank ileal NET. Tryptophan can be either transformed into N'-formylkynurenine by the indoleamine 2,3-dioxygenase leading to L-kynurenine and its derivatives that have anti-fibrotic and anti-inflammatory properties or into 5-hydroxytryptophan by the tryptophan hydroxylase followed by decarboxylation to serotonin by the aromatic l-amino acid decarboxylase serotonin through multiple steps¹³. The balance between the two pathways controls the serotonin production. A correlation between serotonin production and fibrotic disease have been discussed in pulmonary, cardiac or liver fibrosis, which are more frequent if patients have carcinoid syndromes¹²⁻¹⁵. In these diseases, TGF- β was upregulated¹⁸. It was also well demonstrated in multiple wound repair models that serotonin activates fibroblasts leading to extra cellular matrix deposition and further TGF- β -dependent paracrine activation¹³.

The two main enzymes involved in serotonin production were indeed increased in SP-PanNET (Fig. 3c). Accordingly, we also found increased TGF- β signatures in SP-PanNET together with extra cellular matrix remodeling. We could reproduce these signatures in vitro on immortalized pancreatic stellate cells exposed to serotonin suggesting that serotonin is responsible for their activation, proliferation and matrix deposition. It should be noted that this in vitro work has several limitations. First the pancreatic fibroblasts that were used were not naïve stellate cells but immortalized and cultured on plastic with may alter their response to external stimuli. In addition, these cells were treated with recombinant serotonin at a dose in accordance with other publications in the tissue repair field and in the fluids of patient with ileal NET but we cannot be certain that this concentration is indeed present in SP-PanNET, in which paracrine stimulation may require lower amount of serotonin⁴¹.

In routine practice, when faced with a serotonin producing NET located in the pancreas in a patient with a synchronic or metachronous ileal SP-NET, the question of whether this is a primary or metastatic tumor is frequent. This is an important distinction as pancreatic NET and their ileal counterparts do not have the same prognosis and do not share the same therapeutic arsenal. Expression of classical ileal NET markers such as serotonin, CDX2 and the absence of NF-PanNET marker such as ISLET1 and abnormal MENIN, DAXX, ATRX staining may be misleading. Here, we propose that PDX1 and to a lesser extent PAX6 could be useful tools to distinguish SP-PanNET from pancreatic ileal NET metastases, an important finding when considering the excellent prognosis of SP-PanNET. It should be noted that the proteins of the PAX family share important homology leading to potential cross-reaction with some antibodies, especially the polyclonal ones. We chose to use a PAX6 antibody (and not a more widely available PAX8 antibody) as RNA expression data showed that PAX8 is not expressed or at a very low level in normal endocrine cells and PanNET (personal data and single cell data from the Human Atlas repository, not shown)⁴². The reported PAX8 positivity of PanNET is most likely due to antibody cross-reactivity. Pathologist should therefore be careful when choosing their PAX family antibodies.

In conclusion, SP-PanNET are rare pancreatic tumors with fairly similar microscopic and immunohistochemical appearance compared to ileal NET. However, their genomic profile is distinct from ileal NET, but also from NF-PanNET. Biologically, SP-PanNET are also unique, displaying an exclusive beta-like profile but with a serotonin-mediated activation of pancreatic stellate cell leading to the extensive extra cellular matrix deposition.

DATA AVAILABILITY

Original genomic and transcriptomic files will be available from the corresponding author upon request.

REFERENCES

- Peart, W. S., Porter, K. A., Robertson, J. I., Sandler, M. & Baldock, E. Carcinoid syndrome due to pancreatic-duct neoplasm secreting 5-hydroxytryptophan and 5-hydroxytryptamine. *Lancet* **1**, 239–243 (1963).
- Modlin, I. M., Lye, K. D. & Kidd, M. A 5-decade analysis of 13,715 carcinoid tumors. *Cancer* **97**, 934–959 (2003).
- Lloyd, R. V., Osamura, R. Y., Kloppel, G. & Rosai, J. WHO Classification of Tumours of Endocrine Organs. 4th Edition (2017).
- Kalhor, N., Suster, S. & Moran, C. A. Primary Sclerosing Neuroendocrine Carcinomas of the Lung: A Clinicopathologic and Immunohistochemical Study of 10 Cases. *Am. J. Clin. Pathol.* **133**, 618–622 (2010).
- Burgio, M. D. Serotonin immunoreactive pancreatic neuroendocrine neoplasm associated with main pancreatic duct dilation: a recognizable entity with excellent long-term outcome. *Eur. Radiol.* **11**, 8671–8681 (2021).
- Kawamoto, S., Shi, C., Hruban, R. H., Choti, M. A., Schulick, R. D., Fishman, E. K. et al. Small serotonin-producing neuroendocrine tumor of the pancreas associated with pancreatic duct obstruction. *Am. J. Roentgenol.* **197**, W482–W488 (2011).

- Scott, A. T., Pelletier, D., Maxwell, J. E., Sherman, S. K., Keck, K. J., Li, G. et al. The pancreas as a site of metastasis or second primary in patients with small bowel neuroendocrine tumors. *Ann. Surg. Oncol.* **26**, 2525–2532 (2019).
- Australian Pancreatic Cancer Genome Initiative, Scarpa, A., Chang, D. K., Nones, K., Corbo, V., Patch, A.-M. et al. Whole-genome landscape of pancreatic neuroendocrine tumours. *Nature* **543**, 65–71 (2017).
- Scarpa, A. The landscape of molecular alterations in pancreatic and small intestinal neuroendocrine tumours. *Annales d'Endocrinologie* **80**, 153–158 (2019).
- La Rosa, S., Franzini, F., Albarello, L., Schmitt, A., Bernasconi, B., Tibiletti, M. G. et al. Serotonin-producing enterochromaffin cell tumors of the pancreas: clinicopathologic study of 15 cases and comparison with intestinal enterochromaffin cell tumors. *Pancreas* **40**, 883–895 (2011).
- Blažević, A., Hofland, J., Hofland, L. J., Feelders, R. A. & de Herder, W. W. Small intestinal neuroendocrine tumours and fibrosis: an entangled conundrum. *Endocr. Relat. Cancer* **25**, R115–R130 (2018).
- Bader, M. Inhibition of serotonin synthesis: A novel therapeutic paradigm. *Pharmacol. Ther.* **205**, 107423 (2020).
- Dolivo, D. M., Larson, S. A. & Dominko, T. Tryptophan metabolites kynurenine and serotonin regulate fibroblast activation and fibrosis. *Cell. Mol. Life Sci.* **75**, 3663–3681 (2018).
- Zhang, J., Cui, R., Feng, Y., Gao, W., Bi, J., Li, Z. et al. Serotonin exhibits accelerated bleomycin-induced pulmonary fibrosis through tph1 knockout mouse experiments. *Med. Inflamm.* **2018**, 1–10 (2018).
- Oga, T., Matsuoka, T., Yao, C., Nonomura, K., Kitaoka, S., Sakata, D. et al. Prostaglandin F_{2a} receptor signaling facilitates bleomycin-induced pulmonary fibrosis independently of transforming growth factor- β . *Nat. Med.* **15**, 1426–1430 (2009).
- Laskaratos, F., Rombouts, K., Caplin, M., Toumpanakis, C., Thirlwell, C. & Mandair, D. Neuroendocrine tumors and fibrosis: An unsolved mystery? *Cancer* **123**, 4770–4790 (2017).
- Johnson, A., Wright, J. P., Zhao, Z., Komaya, T., Parikh, A., Merchant, N. et al. Cadherin 17 is frequently expressed by 'sclerosing variant' pancreatic neuroendocrine tumour. *Histopathology* **66**, 225–233 (2015).
- Biernacka, A., Dobaczewski, M. & Frangogiannis, N. G. TGF- β signaling in fibrosis. *Growth Factors* **29**, 196–202 (2011).
- Budi, E. H., Schaub, J. R., Decaris, M., Turner, S. & Derynck, R. TGF- β as a driver of fibrosis: physiological roles and therapeutic opportunities. *J. Pathol.* **254**, 358–373 (2021).
- McCall, C. M., Shi, C., Klein, A. P., Konukiewicz, B., Edil, B. H., Ellison, T. A. et al. Serotonin expression in pancreatic neuroendocrine tumors correlates with a trabecular histologic pattern and large duct involvement. *Human Pathology* **43**, 1169–1176 (2012).
- Inzani, F., Petrone, G. & Rindi, G. The new world health organization classification for pancreatic neuroendocrine neoplasia. *Endocrinol. Metab. Clin. North Am.* **47**, 463–470 (2018).
- Piqueret-Stephan, L., Marcaillou, C., Reyes, C., Honoré, A., Letexier, M., Gentien, D. et al. Massively parallel DNA sequencing from routinely processed cytological smears. *Cancer Cytopathol.* **124**, 241–253 (2016).
- 1000 Genomes Project Consortium, Auton, A., Brooks, L. D., Durbin, R. M., Garrison, E. P., Kang, H. M. et al. A global reference for human genetic variation. *Nature* **526**, 68–74 (2015).
- Lek, M., Karczewski, K. J., Minikel, E. V., Samocha, K. E., Banks, E., Fennell, T. et al. Analysis of protein-coding genetic variation in 60,706 humans. *Nature* **536**, 285–291 (2016).
- Kircher, M., Witten, D. M., Jain, P., O'Roak, B. J., Cooper, G. M. & Shendure, J. A general framework for estimating the relative pathogenicity of human genetic variants. *Nat. Genet.* **46**, 310–315 (2014).
- Jagadeesh, K. A., Wenger, A. M., Berger, M. J., Guturu, H., Stenson, P. D., Cooper, D. N. et al. M-CAP eliminates a majority of variants of uncertain significance in clinical exomes at high sensitivity. *Nat. Genet.* **48**, 1581–1586 (2016).
- Metsalu, T. & Vilo, J. ClustVis: a web tool for visualizing clustering of multivariate data using Principal Component Analysis and heatmap. *Nucleic Acids Res.* **43**, W566–570 (2015).
- Love, M. I., Huber, W. & Anders, S. Moderated estimation of fold change and dispersion for RNA-seq data with DESeq2. *Genome Biol.* **15**, 550 (2014).
- Subramanian, A., Tamayo, P., Mootha, V. K., Mukherjee, S., Ebert, B. L., Gillette, M. A. et al. Gene set enrichment analysis: a knowledge-based approach for interpreting genome-wide expression profiles. *Proc. Natl. Acad. Sci. USA* **102**, 15545–15550 (2005).
- Froeling, F. E. M., Mirza, T. A., Feakins, R. M., Seedhar, A., Elia, G., Hart, I. R. et al. Organotypic Culture Model of Pancreatic Cancer Demonstrates that Stromal Cells Modulate E-Cadherin, β -Catenin, and Ezrin Expression in Tumor Cells. *Am. J. Pathol.* **175**, 636–648 (2009).
- Guedj, N., Blaise, L., Cauchy, F., Albuquerque, M., Soubrane, O. & Paradis, V. Prognostic value of desmoplastic stroma in intrahepatic cholangiocarcinoma. *Mod Pathol* **34**, 408–416 (2021).

32. Soga, J., Tazawa, K. Pathologic analysis of carcinoids Histologic reevaluation of 62 cases. *Cancer*. **28**, 990-8 (1971).
33. Pea, A., Yu, J., Marchionni, L., Noe, M., Luchini, C., Pulvirenti, A. et al. Genetic analysis of small well-differentiated pancreatic neuroendocrine tumors identifies subgroups with differing risks of liver metastases. *Ann. Surg.* **271**, 566–573 (2020).
34. Wang, H., Bender, A., Wang, P., Karakose, E., Inabnet, W. B., Libutti, S. K. et al. Insights into beta cell regeneration for diabetes via integration of molecular landscapes in human insulinomas. *Nat. Commun.* **8**, 767 (2017).
35. Cho, S.-J., Yoon, C., Lee, J. H., Chang, K. K., Lin, J., Kim, Y.-H. et al. *KMT2C* Mutations in diffuse-type gastric adenocarcinoma promote epithelial-to-mesenchymal transition. *Clin. Cancer Res.* **24**, 6556–6569 (2018).
36. Chen, X., Zhang, G., Chen, B., Wang, Y., Guo, L., Cao, L. et al. Association between histone lysine methyltransferase *KMT2C* mutation and clinicopathological factors in breast cancer. *Biomed. Pharmacother.* **116**, 108997 (2019).
37. Ishida, S., Akita, M., Fujikura, K., Komatsu, M., Sawada, R., Matsumoto, H. et al. Neuroendocrine carcinoma and mixed neuroendocrine–non-neuroendocrine neoplasm of the stomach: a clinicopathological and exome sequencing study. *Human Pathol.* **110**, 1–10 (2021).
38. Almaça, J., Molina, J., Menegaz, D., Pronin, A. N., Tamayo, A., Slepak, V. et al. Human beta cells produce and release serotonin to inhibit glucagon secretion from alpha cells. *Cell Reports* **17**, 3281–3291 (2016).
39. Makhmutova, M., Weitz, J., Tamayo, A., Pereira, E., Boulina, M., Almaça, J. et al. Pancreatic β -cells communicate with vagal sensory neurons. *Gastroenterology* **160**, 875-888. e11 (2021).
40. Moon, J. H., Kim, H., Kim, H., Park, J., Choi, W., Choi, W. et al. Lactation improves pancreatic β cell mass and function through serotonin production. *Sci. Transl. Med.* **12**, eaay0455 (2020).
41. Onaitis, M. W., Kirshbom, P. M., Hayward, T. Z., Quayle, F. J., Feldman, J. M., Seigler, H. F. et al. Gastrointestinal carcinoids: characterization by site of origin and hormone production. *Ann. Surg.* **232**, 549–556 (2000).
42. Tacha, D., Qi, W., Zhou, D., Bremer, R. & Cheng, L. PAX8 mouse monoclonal antibody [BC12] recognizes a restricted epitope and is highly sensitive in renal cell and ovarian cancers but does not cross-react with b cells and tumors of pancreatic origin. *Appl. Immunohistochem. Mol. Morphol.* **21**, 59–63 (2013).

ACKNOWLEDGEMENTS

We would like to thank Sandrine Tessiere, Nathalie Colnot, Karl Lhuissier et Gaëlle Picard for their technical support.

AUTHOR CONTRIBUTIONS

J.C. performed study concept and design; T.D., R.L. and J.C. performed development of methodology and writing, review and revision of the paper; T.D., R.L., D.A., R.N., M. N. and A.P. provided acquisition, analysis and interpretation of data, and statistical analysis; S.D., P.R., O.H., L.d.M., V.P. and A.C. provided technical and material support. All authors read and approved the final paper.

COMPETING INTERESTS

The authors declare no competing interests.

ETHICAL APPROVAL

This study was performed according to Helsinki declaration. The study was approved by local Institutional Review Board (CEERB Paris Nord, IRB 00006477-15-073).

ADDITIONAL INFORMATION

Supplementary information The online version contains supplementary material available at <https://doi.org/10.1038/s41379-022-01110-x>.

Correspondence and requests for materials should be addressed to Jérôme Cros.

Reprints and permission information is available at <http://www.nature.com/reprints>

Publisher's note Springer Nature remains neutral with regard to jurisdictional claims in published maps and institutional affiliations.